International Journal of Nanoelectronics and Materials
IJNeaM
ISSN 1985-5761 | E-ISSN 2232-1535

Effect of Pulsed Laser on Deposition of Graphene Layers on Silicon (N-P) Substrates and Studying their Physical Properties: An Experimental Study

Shareef Faiq Sultan Al-Tikrity*, Athraa Nazar Taha

Department of Physics, College of Science, Tikrit University, Salah al-din, Iraq
**Corresponding author. Tel.: +964 7738205015; E-mail: ashareef.ph.sc@tu.edu.au, athraa.n.taha.phys576@st.tu.edu.iq*

ABSTRACT

In this research, the effect of a pulsed laser at 100 pulses was studied on graphene layers deposited on n-type and p-type silicon substrates using spin coating technique. The effect of laser pulses on the reduction of graphene layers was observed, which was clearly demonstrated in AFM images, where a decrease in the thickness of the graphene layer was observed after laser treatment. From XRD results of the samples before and after treatment, a noticeable decrease in the intensity of graphene after exposure to laser pulses appeared. FESEM images of graphene samples deposited on silicon (N-P) substrates are also shown. The samples appear as scattered wrinkled flakes with a crystalline size ranging from (98-78) nm. After laser irradiation, the wrinkled flakes appear in smooth layers evenly distributed on the surface, with the crystalline size decreasing to (66-54) nm. FTIR spectra show vibrational groups of graphene including carbonyl (C=O), aromatic (C=C), carboxyl (COOH), epoxy (CO-C), and hydroxyl (OH) groups" it should be "carbonyl (C=O), (C=C), carboxyl (COOH), epoxy (CO-C), and hydroxyl (OH) groups. Photoluminescence spectroscopy was also used to calculate the energy gap, and its value was observed to decrease after laser irradiation. These results are important for optoelectronic devices due to the distinctive properties resulting from the reduction of the graphene layers obtained. FESEM images of graphene samples deposited on silicon (N-P) substrates are also shown. The samples appear as scattered wrinkled flakes with a crystalline size ranging from (98-78) nm.

Keywords: *Silicon (N-P), Graphene, Pulsed laser, XRD, FESEM*

1. INTRODUCTION

Nanocarbons possess a multi-dimensional structure, such as fullerene in zero-dimension, carbon nanotubes in one dimension, and graphene in two dimensions, offering significant promise in a wide range of applications, including electrocatalysis, sensing, bio-imaging, and more. Among them, graphene has attracted widespread attention since its discovery in 2004 [1]. Graphene is an atomic thin sheet of one or a few carbon atoms, hybridized with sp^2 in a two-dimensional honeycomb lattice[2-4]. Graphene has been widely studied and shown to have unique properties such as large surface area (~2600 m^2/g), high electron mobility (200,000 $cm^2/V.s$), enhanced thermal conductivity (3000-5000 W/m.K), extreme optical transparency (97.4%), and exceptional mechanical strength, with Young's modulus 1TPa and intrinsic strength of 130 GPa[5-6]. The process of producing high-quality graphene with a low number of layers remains a major challenge, despite extensive research efforts. The main hurdle is overcoming the strong van der Waals forces that bind the graphite layers together, making it difficult to isolate individual graphene sheets. Although methods based on chemical or thermal treatments have been proposed to reduce the number of layers and improve the quality of graphene. However, chemical treatments rely on toxic and dangerous materials, while thermal treatments require high temperatures and different environments [7-9]. Structural defects and impurities may often arise when using these methods, so it was necessary to resort to improving manufacturing methods to obtain the required properties of graphene [9-11]. Recently, the method of laser reduction of graphene layers has attracted attention because it is an easy, safe and fast method as well, as it takes only a few minutes and with its high accuracy. It can be used to assemble or modify graphene films and to directly manufacture electronic devices with improved properties. The number of graphene layers and the degree of graphene reduction can be controlled by adjusting various laser parameters such as frequency and number of pulses[12-14]. On the other hand, differences in conductivity between N-type and P-type silicon are critical in the resolve and design of electronics and optoelectronics devices. it is possible to create transistors, and other electronic components that use these differences in conductivity to control the flow of current [15]. In this research, the deposition of graphene on silicon by spin coating and processing of the prepared films with pulsed laser was studied to obtain thin layer graphene films for use in optics and electronic devices.

2. MATERIALS AND METHODS

2.1. Preparation of Graphene Films

Spin coating method was employed to prepare the films. The graphene solution was prepared using graphene platelets nanopowder (Skyspring nanomaterials, USA), ethanol (96%) and stearic acid ((C18H36O2); HIMEDIA, India) was utilized as the bonding material between the solute and solvent. First, (0.005gm) of stearic acid was dissolved in (50

ml) of ethanol under continuous magnetic stirring and heating on a hot plate stirrer. After it dissolved completely, (0.250 gm) of graphene was added to solution and continued stirring and heating for 5 minutes to yield a clear and homogeneous solution. The final solution served as the coating source after cooling down to room temperature. Before deposition, the silicon substrates were successively cleaned using acetone, ethanol, and deionized water and then dried. Graphene thin films were deposited on n-type and p-type silicon substrates by spin coating at room temperature. The coating solution was dropped into the cleaned silicon substrates fixed at the top base of the spin coating unit, which was rotated at 3000 rpm for 30 s. Then, all the films were dried at 70°C for 10 minutes to allow for the evaporation of the solvent and binder.

2.2. Laser Films Treatment

The prepared graphene films were processed by a pulsed Nd: YAG laser. At an energy of (300 mJ), a pulse frequency of (60 Hz), and a wavelength of (1064 nm), with 100 pulses. Laser irradiation was carried out in normal atmospheric conditions.

3. RESULTS AND DISCUSSION

3.1. Structural Properties

Figure 1 shows the X-ray diffraction pattern of graphene films deposited by spin coating on n-type and p-type silicon. The figure shows the appearance of a peak of high intensity at a diffraction angle of 69° and a crystallographic plane (100). In addition, it showed another peak at an angle of 26.6° with a crystallographic plane (002) which belonged to graphene according to (JCPDS card No:96-120-0019). This is the preferred direction of graphene and is constant in the graphene and carbon structure of the hexagonal lattice. The full width of the middle of the graphene peak with the dominant orientation (002) was determined. In addition, the Crystallite size was calculated and the values of d-spacing and micro strain were given with X-ray examination. As shown in Table 1.

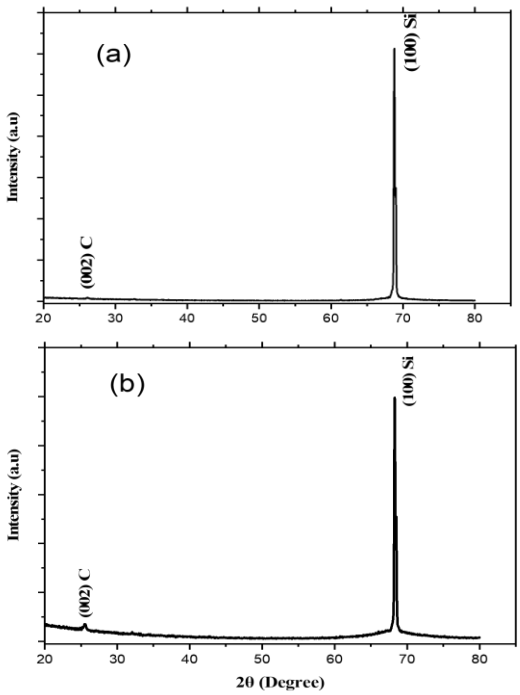

Figure 1. XRD patterns of graphene prepared films deposited on (a) n-type silicon (b) p-type silicon.

When graphene is treated with 100 laser pulses, it is noted that the intensity of the graphene peak decreased as a result of reducing the thickness of graphene layers from the Si-substrate. It is also noted that the peak shifted slightly as a result of the decrease in crystalline size and the change in lattice strain values as show in Figure 2.

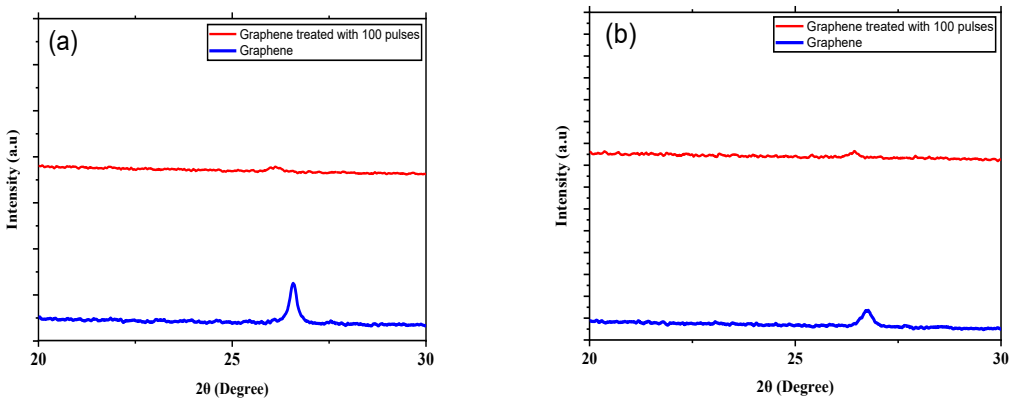

Figure 2. Diffraction peaks of graphene after treatment with 100 laser pulses (a) graphene deposited on n-type silicon. (b) graphene deposited on p-type silicon.

Table 1 Structural parameters of graphene thin films deposited on n-type and p-type silicon

Substrate type	Laser pulses	2θ (Deg.)	FWHM (Deg.)	d-spacing (Å)	Crystallite Size (D) (nm)	Micro Strain (ε)	hkl
n-type	0	26.5523	0.1826	3.35431	78.09	0.43037	(002)
	100	26.0023	0.2831	3.42399	54.84	0.81527	(002)
p-type	0	26.7098	0.4141	3.33488	98.44	1.1425	(002)
	100	26.4314	6.0524	3.23797	66.45	1.4677	(002)

The thickness of the prepared films was calculated using an atomic force microscope, and it was found that the number of graphene layers decreased after laser irradiation, as shown in Table 2. Graphene nanoparticles were applied to two types of substrates (P-N) before being irradiated with laser as in Figure 3 and at 100 pulses and imaged by AFM as shown in Figure 4. It was found that the AFM results are affected by the type of substrate, shape, behavior and surface nature of the nanoparticles and the nanoparticle solution used. It was also observed that the surface of the samples was affected by the laser energy and the number of pulses, which led to the surface peeling and homogeneity as a result of etching when the number of pulses increased. The appearance of grains and pits was also observed on the P substrate. As for N substrate, we notice clear roughness on the surface.

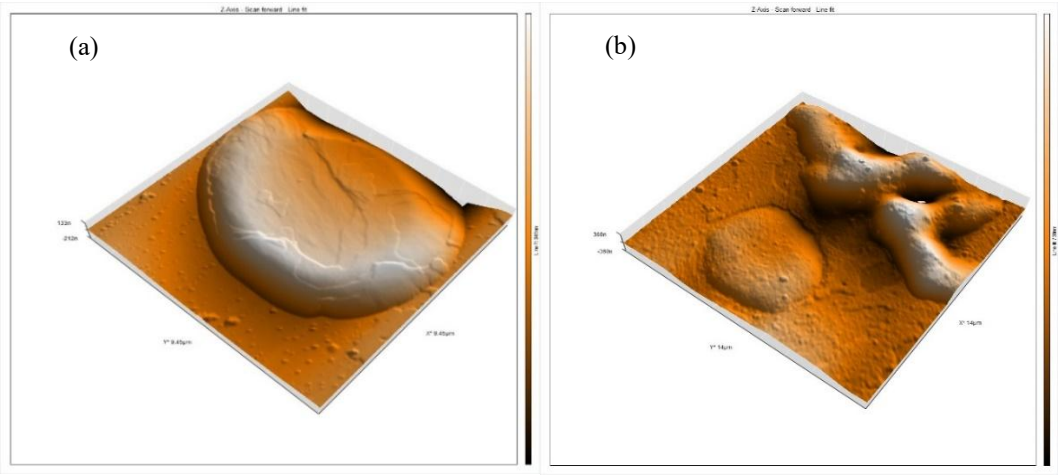

Figure 3. AFM-3D images of Graphene deposited on n-type silicon. (a) graphene before laser treatment. (b) graphene after irradiation with 100 pulses.

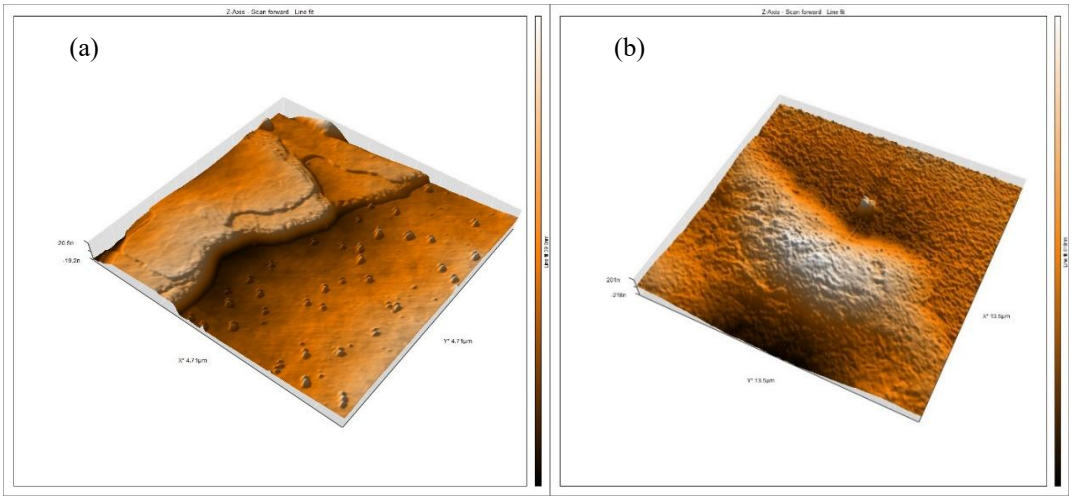

Figure 4. AFM-3D images of Graphene deposited on p-type silicon. (a) graphene before laser treatment. (b) graphene after irradiation with 100 pulses.

Table 2 Thickness of graphene films deposited on n-type and p-type silicon substrates before and after laser treatment

Substrate type	Number of pulses	Thickness (nm)
n-type	0	119.3
	100	22.79
p-type	0	41.43
	100	8.223

3.2. Surface Morphology and Compositional Analysis

The surface morphology of graphene films deposited on n-type and p-type silicon substrates before and after laser treatment was analyzed using FESEM technology.

Figure 5 shows FESEM images of graphene samples deposited on n-type silicon substrates. Fig.5a samples before laser treatment and Fig.5b samples after treatment with 100 pulses. The surface of graphene film appeared in the form of scattered flakes, and after treating with a laser, it became more consistent and smoother, with some cracks as a result of direct laser energy concentration, and the particle size decreasing from (78-54) nm. Figure 6 shows FESEM images of graphene samples deposited on p-type silicon substrates. The samples appear as compact, wrinkled flakes with a particle size of 98 nm. When irradiated with a laser, a mixture of granules and wrinkled flakes appears. Smooth and complete graphene layers are clearly formed and evenly distributed on the surface with a particle size of 66 nm. It is concluded from here that the size of the particles decreases after laser irradiation.

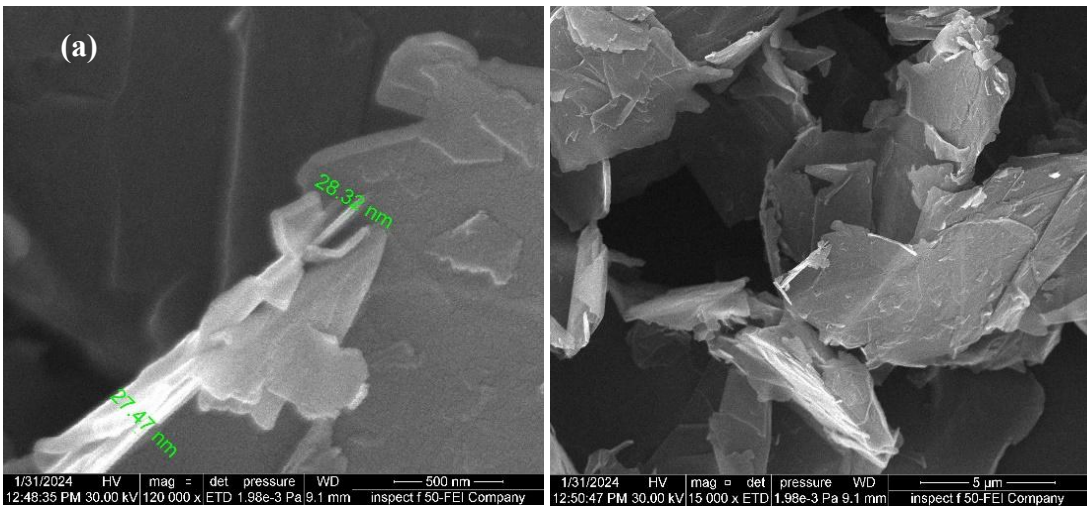

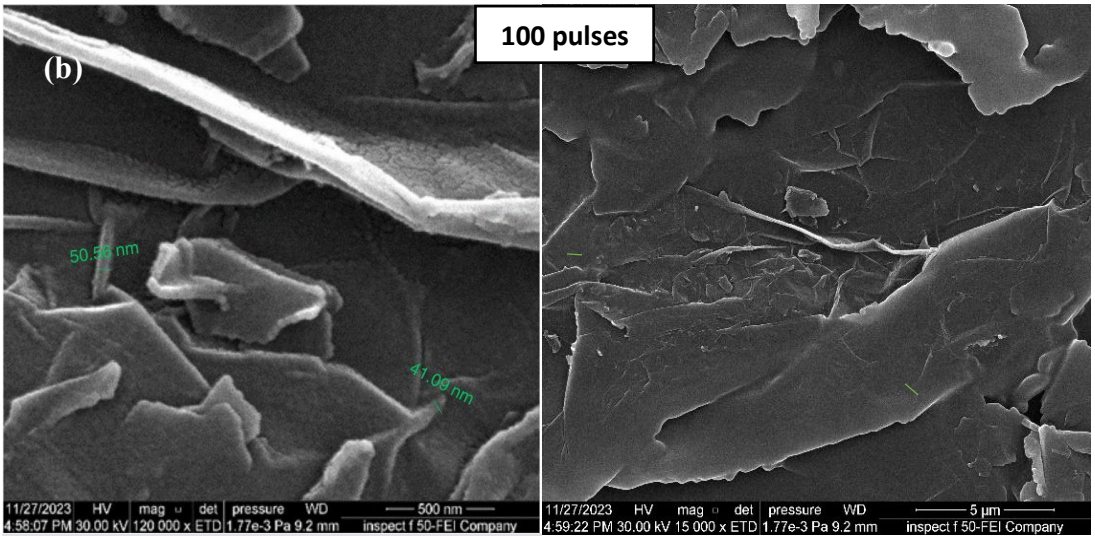

Figure 5. FESEM images of graphene films deposited on n-type silicon (a) graphene before laser treatment. (b) with 100 pulses.

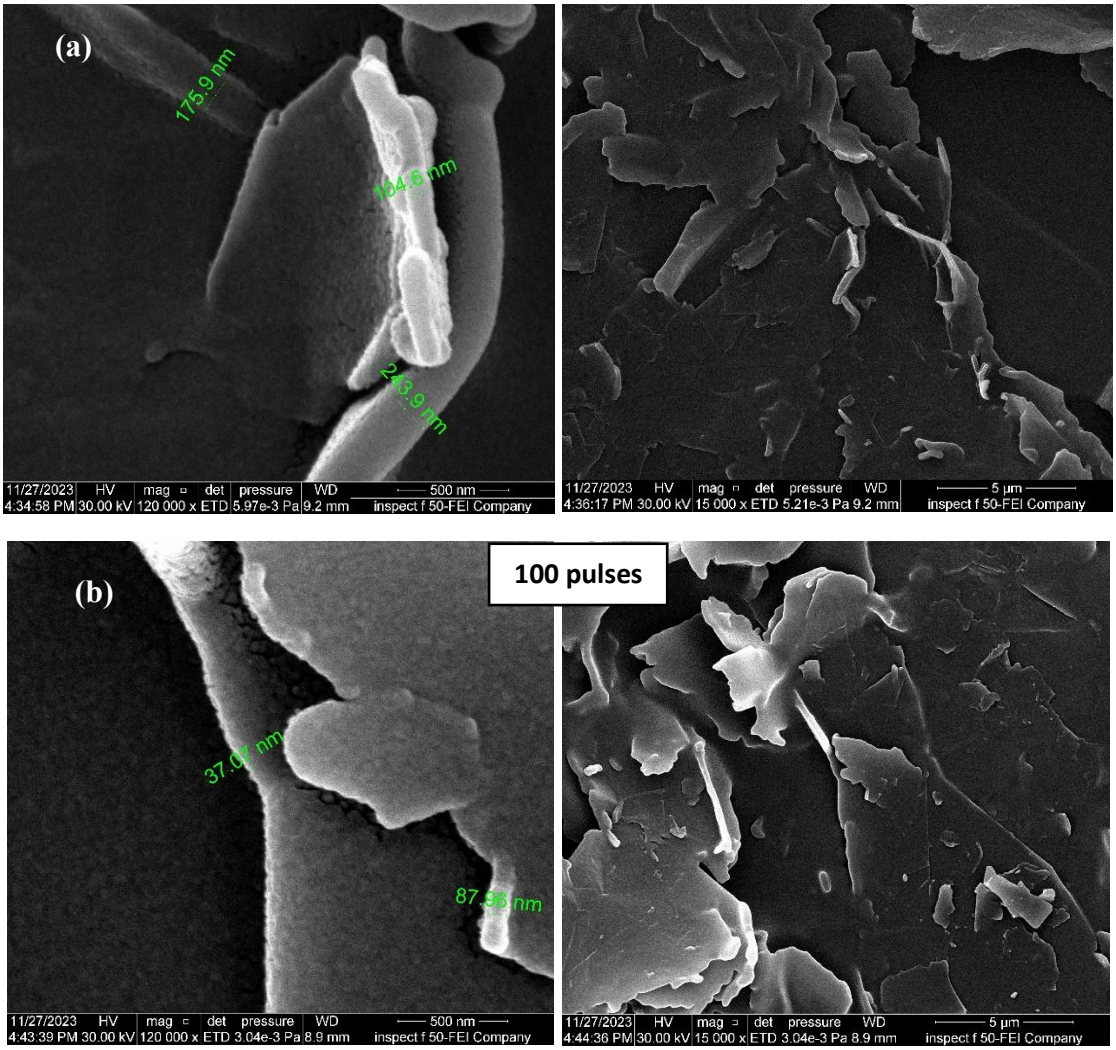

Figure 6. FESEM images of graphene films deposited on p-type silicon (a) graphene before laser treatment. (b) with 100 pulses.

The weight and atomic percentages were determined by using the energy-dispersive X-ray spectroscopy technique as shown in Table 3. It showed a clear decrease in the percentage of carbon as a result of peeling layers when irradiated with a laser, as well as the percentage of oxygen. It is noticed from figure (7 , 8) that a high peak corresponding to the characteristic emission line of silicon that belonged to the substrate , in addition to the carbon and oxygen peaks.

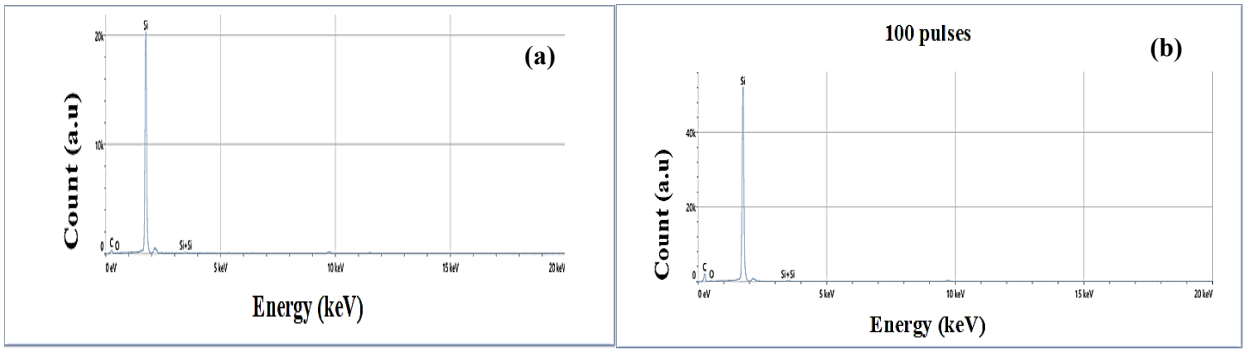

Figure 7. EDX Spectra of Graphene deposited on n-type silicon. (a) graphene before laser treatment. (b) graphene after irradiation with 100 pulses.

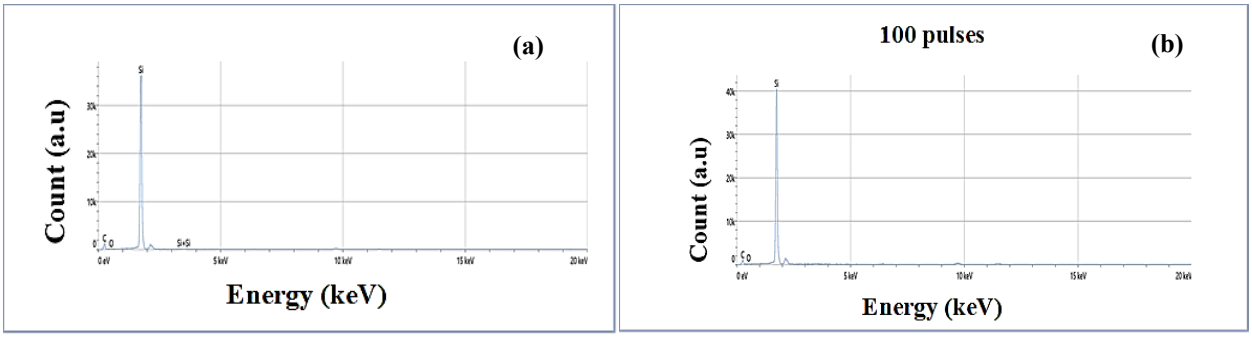

Figure 8. EDX Spectra of Graphene deposited on p-type silicon. (a) graphene before laser treatment. (b) graphene after irradiation with 100 pulses.

Table 3 Comparison between the weight and atomic percentages of graphene samples deposited on n-type and p-type silicon substrates before and after laser treatment

Substrate type	Element	Atomic %	Weight %
Before laser treatment			
n-type	C	46.5	43.7
	O	0.5	0.4
	Si	53.0	72.4
p-type	C	60.0	39.3
	O	0.9	0.8
	Si	39.1	60.0
After laser treatment with 100 puleses			
n-type	C	64.2	27.2
	O	0.9	0.8
	Si	34.9	55.5
p-type	C	54.4	33.9
	O	0.8	0.6
	Si	44.8	65.4

3.3. FTIR Spectra

Figures 9 and 10 showed FTIR spectra within the wavenumber range of (400-4000) cm^{-1} for graphene films deposited on n-type and p-type silicon substrates before and after pulsed laser treatment. Some absorption bands connected with carbonyl compounds with characteristic of graphene are found in FTIR spectrometer. The spectrum consists of multiple vibrational groups including carbonyl (C=O), aromatic (C=C), the stretching vibration of the bond of the carboxylic (COOH), while the band centered at (1256 cm-1) matching to the stretching vibration of the (C–O) bond of epoxy group and hydroxyl (O-H) groups [16] as shown in

Tables 4 and 5. A clear change can be observed in the n-type FTIR spectra due to the strengthening of the (π) bond in graphene (carbon atoms) by reducing defects, which ultimately leads to closing the conduction gap and enhancing electrical conductivity of n-type, in contrast to the p-type, which does not show a significant change [17].

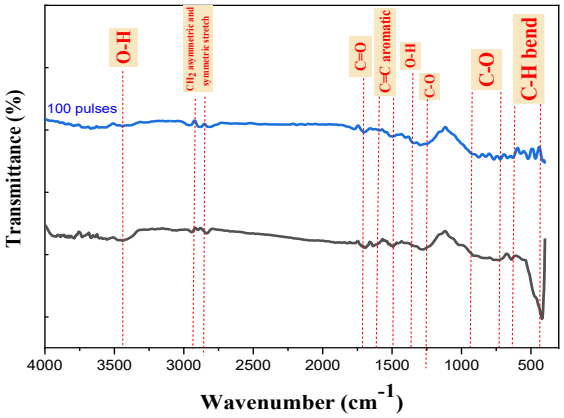

Figure 9. FTIR spectra of graphene samples deposited on n-type silicon substrates before and after laser treatment.

Table 4 Vibrational bands positions for FTIR spectra of graphene samples deposited on n-type silicon substrates before and after pulsed laser treatment

Functional group	**Wave number (cm^{-1})**	
Number of pulses	**None**	**100 Pulses**
O-H	3441.01	3454.51
Asymmetric CH2	2937.59	2914.44
Symmetric CH2	2837.29	2846.93
C=O	1695.43	1693.50
Aromatic C=C	1552.70	1585.49
O-H	1411.89	1367.53
C-O	1271.19	1234.44
	1016.49	1002.98
	912.33	933.55
C-H bend	638.44	574.79
	478.35	493.78

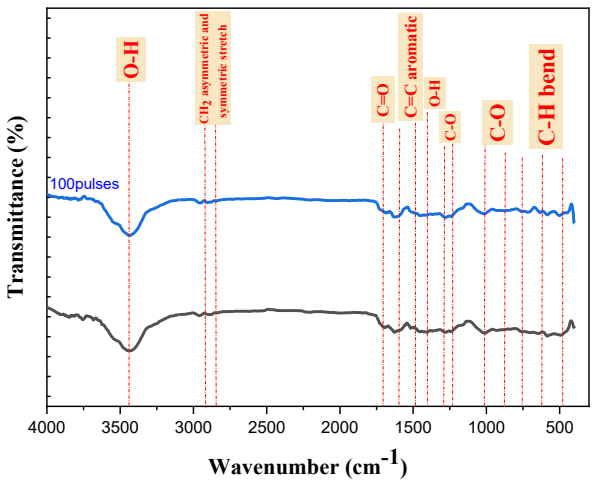

Figure 10. FTIR spectra of graphene samples deposited on p-type silicon substrates before and after laser treatment.

Table 5 Vibrational bands positions for FTIR spectra of graphene samples deposited on p-type silicon substrates before and after pulsed laser treatment

Functional group	**Wave number (cm^{-1})**	
Number of pulses	**None**	**100 Pulses**
O-H	3442.94	3439.08
Asymmetric CH2	2960.73	2954.95
Symmetric CH2	2873.94	2912.51
C=O	1703.14	1693.50
Aromatic C=C	1622.13	1627.92
	1460.11	1450.47
O-H	1375.25	1369.46
C-O	1008.77	1010.70
	931.62	846.75
C-H bend	754.17	756.10
	584.43	580.57
	489.92	493.78

3.4. PL Spectroscopy

Photoluminescence spectroscopy was used to calculate the energy gap value of graphene films according to the energy gap equation, which is [18]:

$$E_g = \frac{1240}{\lambda}$$

Where λ represents the highest peak of wavelength. As Figure 11 shows., there are two prominent peaks the high peak within the wavelength range of 520-560 nm belonged to graphene, while the second peak which is slightly smaller in the range 260-280 nm belonged to silicon substrates. Table 8 shows the energy gap values. The band gap of graphene varies depending on the oxygen groups present in the structure. The decrease in the oxygen-bound group may allow energy gap values to be controlled using the type of substrate and determining the pulse energy and number upon laser treatment applied, which is consistent with Ref. [19-20].

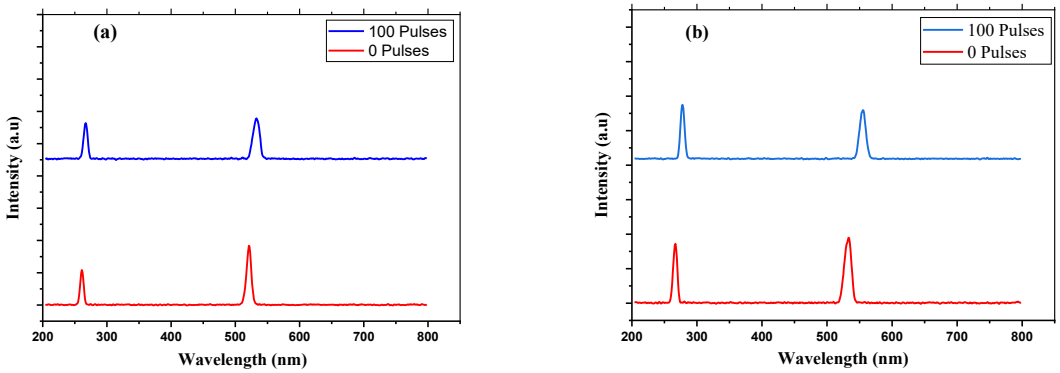

Figure 11. PL spectra of graphene samples deposited on (a) n-type (b) p-type silicon substrates before and after laser treatment.

Table 6 Energy gap values of graphene samples deposited on n-type and p-type silicon substrates

Substrate type	**Number of pulses**	**wavelength (nm)**	**E_g (eV) graphene**	**wavelength (nm)**	**E_g (eV) silicon**
n-type	0	521.94	2.38	260.92	4.75
	100	532.05	2.33	265.93	4.66
p-type	0	533.97	2.32	265.93	4.66
	100	556.02	2.23	277.07	4.48

4. CONCLUSION

Studying graphene on layers of silicon and treating it with a pulsed laser is considered one of the most important techniques that seek to obtain few layers of graphene deposited on a silicon substrate of two types of silicon (N and P), characterized by an ordered and homogeneous structure for use in optoelectronic devices. Where a group of graphene layers were scraped to obtain good conductivity of the graphene and reduce the graphene layers. Its surface and morphological properties were also improved by applying pulsed laser treatment the deposited film. The chemical bonds were also improved and areas were obtained to strengthen the bonding of the graphene molecules due to increased surface area of the samples and reduced particles size. Based on the results obtained, the pulsed laser method can be used as a good method to reduce the graphene layers. Using this method is clean and inexpensive, preserves the crystalline structure of graphene and does not cause significant defects or distortions on the surfaces of the samples. So, these results are very important for improving the structural and optical properties of devices used in communications, scanning devices, and storage device

REFERENCES

[1] Y. Zhao, Q. Han, Z. Cheng, L. Jiang, and L. Qu, "Integrated graphene systems by laser irradiation for advanced devices," Nano Today, vol. 12. Elsevier B.V., pp. 14–30, Feb. 01, 2017. doi: 10.1016/j.nantod.2016.12.010.

[2] A. Torrisi, L. Velardi, A. Serra, D. Manno, L. Torrisi, and L. Calcagnile, "Graphene oxide modifications induced by excimer laser irradiations," Surface and Interface Analysis, vol. 54, no. 5, pp. 567–575, May 2022, doi: 10.1002/sia.7066.

[3] Xiao, Y., Pang, Y. X., Yan, Y., Qian, P., Zhao, H., Manickam, S., Wu, T., & Pang, C. H., "Synthesis and Functionalization of Graphene Materials for Biomedical Applications: Recent Advances, Challenges, and Perspectives," Advanced Science, vol. 10, no. 9. John Wiley and Sons Inc, Mar. 24, 2023. doi: 10.1002/advs.202205292.

[4] S. Sultan,., C. Zhang, "Nonlinear optical conductance of a gapped graphene p-n junction in THz regime" International Conference on Infrared, Millimeter, and Terahertz Waves, IRMMW-THz, 2012, 6380394.

[5] K. S. Novoselov, V. I. Fal'Ko, L. Colombo, P. R. Gellert, M. G. Schwab, and K. Kim, "A roadmap for graphene," Nature, vol. 490, no. 7419. pp. 192–200, Oct. 11, 2012. doi: 10.1038/nature11458.

[6] A. R. Urade, I. Lahiri, and K. S. Suresh, "Graphene Properties, Synthesis and Applications: A Review," JOM, vol. 75, no. 3. Springer, pp. 614–630, Mar. 01, 2023. doi: 10.1007/s11837-022-05505-8.

[7] Z. S. Wu, W. Ren, L. Gao, B. Liu, C. Jiang, and H. M. Cheng, "Synthesis of high-quality graphene with a pre-determined number of layers," Carbon N Y, vol. 47, no. 2, pp. 493–499, Feb. 2009, doi: 10.1016/j.carbon.2008.10.031.

[8] Cooper, D. R., D'Anjou, B., Ghattamaneni, N., Harack, B., Hilke, M., Horth, A., Majlis, N., Massicotte, M., Vandsburger, L., Whiteway, E., & Yu, V., "Experimental Review of Graphene," ISRN Condensed Matter Physics, vol. 2012, pp. 1–56, Apr. 2012, doi: 10.5402/2012/501686.

[9] Backes, C., Abdelkader, A. M., Alonso, C., Andrieux-Ledier, A., Arenal, R., Azpeitia, J., Balakrishnan, N., Banszerus, L., Barjon, J., Bartali, R., Bellani, S., Berger, C., Berger, R., Ortega, M. M. B., Bernard, C., Beton, P. H., Beyer, A., Bianco, A., Bøggild, P., … Garcia-Hernandez, M., "Production and processing of graphene and related materials," 2d Mater, vol. 7, no. 2, Jan. 2020, doi: 10.1088/2053-1583/ab1e0a.

[10] R. Kumar, R. K. Singh, D. P. Singh, E. Joanni, R. M. Yadav, and S. A. Moshkalev, "Laser-assisted synthesis, reduction and micro-patterning of graphene: Recent progress and applications," Coordination Chemistry Reviews, vol. 342. Elsevier B.V., pp. 34–79, Jul. 01, 2017. doi: 10.1016/j.ccr.2017.03.021.

[11] S. Al-Tikrity,, R. Vickers, "Measuring the optical transmittance of graphene with silicon substrates within a particular range of the spectrum from the terahertz to infrared regime" nternational Conference on Infrared, Millimeter, and Terahertz Waves, IRMMW-THz, 2014, 6956249

[12] A. Vasquez, P. Samolis, J. Zeng, and M. Y. Sander, "Micro-structuring, ablation, and defect generation in graphene with femtosecond pulses," OSA Contin, vol. 2, no. 10, p. 2925, Oct. 2019, doi: 10.1364/osac.2.002925.

[13] S. Papazoglou, V. Tsouti, S. Chatzandroulis, and I. Zergioti, "Direct laser printing of graphene oxide for resistive chemosensors," Opt Laser Technol, vol. 82, pp. 163–169, Aug. 2016, doi: 10.1016/j.optlastec.2016.03.009.

[14] Y. Zhou et al., "Microstructuring of graphene oxide nanosheets using direct laser writing," Advanced Materials, vol. 22, no. 1, pp. 67–71, Jan. 2010, doi: 10.1002/adma.200901942.

[15] Y. Xiong, D. Xu, Y. Feng, G. Zhang, P. Lin, and X. Chen, "P-Type 2D Semiconductors for Future Electronics," Advanced Materials, vol. 35, no. 50. John Wiley and Sons Inc, Dec. 14, 2023. doi: 10.1002/adma.202206939.

[16] M. M. Jasim and S. F. S. Al-Tikrity, "Depositing Layers of Nano Graphene on P-Type Silicon Substrate and Studying the Structural and Optical Properties," Journal for Research in Applied Sciences and Biotechnology, vol. 2, no. 5, pp. 83–88, Oct. 2023, doi: 10.55544/jrasb.2.5.13.

[17] M. Bera, Chandravati, P. Gupta, and P. K. Maji, "Facile One-Pot Synthesis of Graphene Oxide by Sonication Assisted Mechanochemical Approach and Its Surface Chemistry," J Nanosci Nanotechnol, vol. 18, no. 2, pp. 902–912, Sep. 2017, doi: 10.1166/jnn.2018.14306.

[18] K. Murawski, M. Kopytko, P. Madejczyk, K. Majkowycz, and P. Martyniuk, "HgCdTe ENERGY GAP DETERMINATION FROM PHOTOLUMINESCENCE AND SPECTRAL RESPONSE MEASUREMENTS," Metrology and Measurement Systems, vol. 30, no. 1, pp. 183–194, 2023, doi: 10.24425/mms.2023.144395.

[19] Witjaksono, G., Junaid, M., Khir, M. H., Ullah, Z., Tansu, N., Saheed, M. S. B. M., Siddiqui, M. A., Ba-Hashwan, S. S., Algamili, A. S., Magsi, 'Effect of nitrogen doping on the optical bandgap and electrical conductivity of nitrogen-doped reduced graphene oxide', Molecules, vol. 26, no. 21, Nov. 2021, doi: 10.3390/molecules26216424.

[20] M. V. Narayana and S. N. Jammalamadaka, 'Tuning Optical Properties of Graphene Oxide under Compressive Strain Using Wet Ball Milling Method', Graphene, vol. 05, no. 02, pp. 73–80, 2016, doi: 10.4236/graphene.2016.52008.